(NASA-CR-199619)

~~(NIPS-95-05614)~~ SMALL SPACECRAFT TECHNOLOGY INITIATIVE (SSTI) Biannual Report, Jan. - Jun. 1995 (TRW) 36 p

N96-13232

Unclas

G3/18 0073251

SMALL SPACECRAFT TECHNOLOGY INITIATIVE (SSTI)

"Progress and Technology Achievement Report"
31 July 1995

NASA Headquarters Contract #NASW-4945

INTRODUCTION AND OVERVIEW

This is the second in a series of semi-annual reports that describe the technology areas being advanced under this contract and the progress achieved to date. The last technology report concentrated on the spacecraft. This report places greater emphasis on the payloads. White papers by several of the payload providers are attached. These are HSI, UCB, PRKE and CAFE. This report covers the period from January 1995 through June 1995.

The SSTI Critical Design Audit (CDA) was conducted on January 17-19, 1995 to review the final designs of the SSTI Flight and Ground System Flight Software and Assembly, Integration and Test plans were reviewed at the Delta CDA held on 15 March 1995. Since January, several meetings have been held at Vandenburg with Lockheed to discuss the launch vehicle/ spacecraft interface and the VAFB range safety requirements.

In February, SSTI program management relocated to Space Park to provide additional program leverage and schedule control. In June, the SSTI program relocated to building M2, at Space Park, for initiation of the Integration and Test Phase of the program.

The program has advanced over the past six months from the requirements development and design phase to the fabrication and test phase. This phase is one of the most critical junctures of spacecraft development. It is typically marked by unexpected technical challenges, which may have far-reaching effects, particularly in the areas of cost and schedule. Five major challenges have occurred in the past six months. A short discussion of each follows:

Solar Cell Costs - The GaAs (16% η) vs. Si (12% η)

A final trade study was performed on solar cell selection in an effort to reduce the solar array weight while meeting cost targets. The GaAs thin film solar cells had an efficiency factor of 16%. This did not meet the manufacturer's target efficiency of 18%. Comparing the GaAs 16% efficiency cells to the Si 12% efficient cells revealed that the GaAs solar cells are still not cost competitive on an installed dollars per watt basis. The lower efficiency Si cells were chosen for the solar array wings. An experimental GaAs patch, which is one part of the ASCE technical demonstration, will be included on the GPS bracket to permit characterization of these cells.

Structure Coupon Tests

As a part of our quality assurance program, the central cylinder was made longer than necessary so that destructive testing could be performed on the excess after it was trimmed from the flight central cylinder. Results from coupon tests were highly scattered (not grouped). An investigation determined that the pre-pregnated material may have been exposed to room temperature longer than recommended. Options discussed included using the central cylinder as-is and fabricating a second central cylinder. Further investigation, including additional coupon testing and an

evaluation of the original design strength requirements, determined that the original central cylinder satisfied the program requirements.

S-Band Receiver Latchup
An on-orbit failure of a Loral receiver indicated a potential problem with our S-Band receiver. In a heavy ion condition, the transponder could latch-up. The only way to re-activate the receiver was via power cycling. In the original SSTI design, the receivers were connected to unswitched power to prevent a relay failure from eliminating a receiver. A review of the design indicated that SSTI could lose both receivers and be unable to recover. A two-step approach was taken to resolve this potential issue. The first step was to move one receiver to switchable power so that recycling would be available if the latch-up occurred. The second to determine the probability of the latch-up. Our study indicated that the potential latchup condition was less than 1 latchup per 50 years per receiver.

Lockheed Load Cycle
The initial testing of the Lockheed launch vehicle showed a rough engine burn which resulted in higher than expected 'g' levels at several points within the spacecraft. Following reviews by TRW and Lockheed, the payload adapter module was modified to eliminate the excess 'g' levels in the spacecraft.

Battery Proof Pressure Test
Two flight cell vessel samples did not pass burst test requirements (Initial burst - 2325 psi, after cycling 2375 psi , specified requirement - 2400 psi.) Because the test results were only slightly below the requirements, battery fabrication continued. Two completed cells were pressure proof tested and failed the requirement of less than 0.005 inch deformation at 1.5 times maximum operating pressure. After review and consultation with VAFB range safety, it was determined that the pressure proof test level could be reduced to 1.25. At this level, the battery cells successfully passed the deformation requirement. The cells will be used as is.

One on-going challenge has been the spacecraft weight and power. This challenge will continue until launch. As each subsystem reports their measured weight and power, the calculated weight and power numbers are adjusted. Weight and power are reported as part of the CCB meetings each week. The spacecraft weight and power remain within their required envelopes.

As we have moved into fabrication of the satellite, we have successful completed several important milestones.

- Completion of the Battery Propulsion Module
- Completion of the dye penetrant inspection of the propulsion tanks
- Completion of random vibration testing for the reaction wheels and torquerods
- Completion of harness definitions for J&T
- Completion of CDAs for DIU, PCU, SAR and DDC at Gulton
- Trained and certified J&T personnel for flight harness manufacturing

The fabrication and test phase of the program has almost been completed. Our next report will focus on the Integration and Test phase of the program.

Appendix 1 - HSI

N15

Airborne and satellite imaging spectrometer development at TRW

Raymond K. De Long, Thomas E. Romesser, Jay Marmo and Mark A. Folkman
TRW Inc., Space and Electronics Group, Redondo Beach, CA 90278

ABSTRACT

TRW has been involved in hyperspectral imaging since late 1989. The first instruments were constructed from commercially available components and were restricted in wavelength response to the visible and near infrared (i.e., about 0.48 micrometers to 0.88 micrometers). They were used to take data from airborne platforms to support phenomenology studies. An instrument was then constructed to make measurements in the SWIR (i.e., out to 2.5 micrometers). It used mostly commercial components and contained some custom developments such as the foreoptics. These early instruments all recorded data using videotape recorders. A real time processor has been constructed which performs real time spectral template matching on six spectral templates. This significantly reduces operator load for systems where spectrally known targets are being sought. We are currently developing three new systems using custom components. The first is a high performance, aircraft based instrument called TRWIS III; the second, called HSI, will be the first hyperspectral imager in space, and is being developed for the NASA Small Satellite Technology Initiative; and the third is an ocean color instrument, known as the Low Resolution Camera, using the hyperspectral approach. Each of these instruments will briefly described.

Keywords: hyperspectral, multi-spectral, imaging, ocean color, remote sensing, sensor, instrument, focal plane array, spectrometer

EARLY GENERATION INSTRUMENTS

TRW Imaging Spectrometers (TRWIS) started in late 1989 as a laboratory experiment using commercially available components including camera lens foreoptics, COTS spectrometers and videotape recorders. The first sensor array used was an intensified CCD type TV camera. The intensifier was used to boost the signal because the spectral channels are narrow so not much signal is available. Even though these cameras can operate at very low light levels, the signal to noise is limited by noise in the intensifier and the tape recorder. The spatial and spectral resolution is limited by the fiber optics coupler between the intensifier and the CCD.

TRWIS B

TRWIS B uses an unintensified CCD camera which became available shortly after we started. It features improved performance and lower cost and has been used extensively for several years. Figure 1 presents a picture of TRWIS B. The characteristics of TRWIS B are presented in Table 1, as are the more recent members of the TRWIS family. The SSTI HSI characteristics are also included.

Table 1 - Performance comparison of TRWIS family & HSI

	TRWIS A	TRWIS B	TRWIS II	TRWIS III	SSTI HSI
Spectral Range (microns)	0.43-0.85	0.46-0.88	1.5-2.5	0.3-2.5	0.4-2.5
Spectral Channels	128	90	108	384	384
Spectral Sampling (nm)	3.3	4.8	12	5 VNIR 6.25 SWIR	5 VNIR 6.38 SWIR
Spatial Pixels	240	240	240	256	256
IFOV (mrad)	1.0	1.0	0.5/1.0	0.9	0.06
TFOV (mrad)	240	240	120/240	230	15.4
Aperture (mm)	1.5	5	17.5/8.5	20	125
Focal Length (mm)	25	25	70/34	70	1048
Focal Ratio	f/16	f/5	f/5	f/3.3	f/8.3
Detectors	Intens. CCD	Si CCD	InSb	CCD / HCT	CCD / HCT
Quantization (bits)	8	8	8	12	12
Recording Media	videotape	videotape	videotape	digital	digital
Year	1990	1991	1992	1995	1996

TRWIS II

TRWIS II was our first attempt to make measurements in the SWIR. It uses a custom IR lens foreoptics, a SPEX 270M spectrometer (repackaged) and a modified commercial InSb camera. The IR focal plane array hybrid is a FLIR camera type array which uses a direct injection readout and has a very large integration capacitor. These two features are less than optimal for hyperspectral applications; however, we were able to get interesting images and valuable experience well in advance of our custom instruments becoming available. Figure 2 presents a picture of TRWIS II. The detector array is cooled with liquid nitrogen. For most of the data collects a vacuum pump was attached to the dewar to cool the array to about 65 k to reduce FPA noise.

Each of these instruments has been flown to collect data. The visible/near IR instruments have been flown extensively in many platforms, both helicopters and prop and jet fixed wing aircraft. Figure 3 presents views of several of the platforms which have hosted TRWIS instruments.

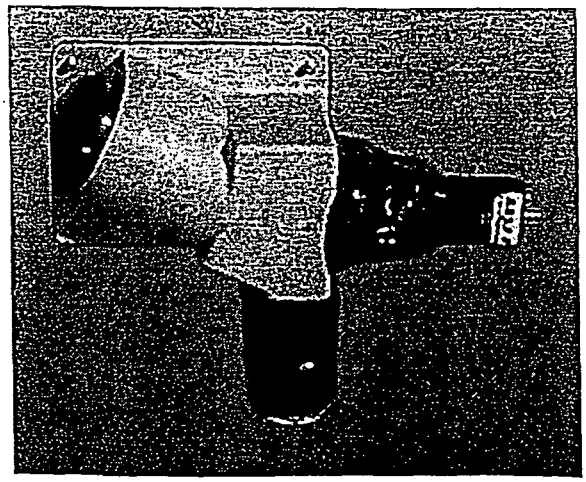

Figure 1 - TRWIS B

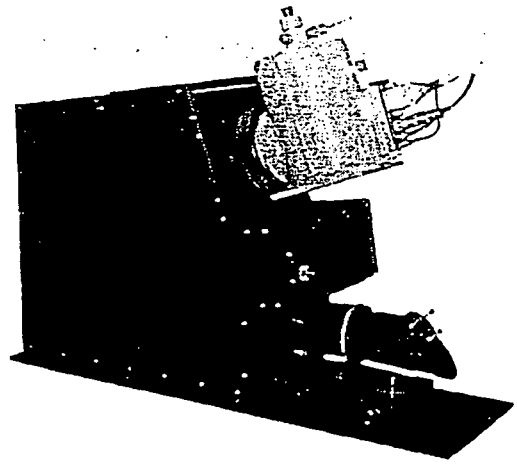

Figure 2 - TRWIS II

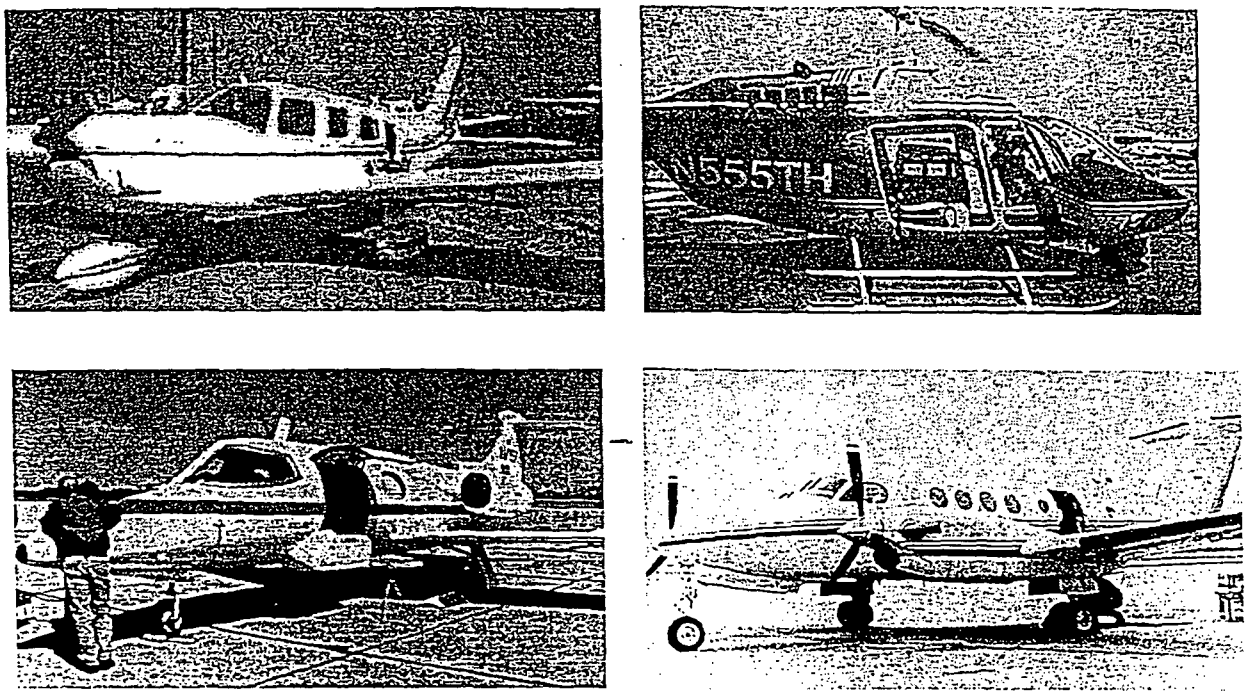

Figure 3 - Platforms used for hyperspectral imaging data collects

NEW DEVELOPMENTS

Our new developments include state of the art airborne and space hyperspectral sensors, known as TRWIS III and HSI respectively, and a new ocean color instrument called the Low Resolution Camera.

TRWIS III

Our new aircraft based instrument is called TRWIS III and is shown in Figure 4 (without focal planes or electronics). It is actually two very similar instruments, covering the VNIR and SWIR bands with overlap from 0.9 to 1.0 micrometers, which are coaligned to have virtually identical fields of view. The refractive elements in the the two instruments are designed and coated specifically for their respective wavelength ranges. The two instruments are designed for very low distortion and for IFOV matching to maintain tight spatial coregistration of spectral channels. TRWIS III has 384 spectral bands (5 nm in the VNIR and 6.25 in the SWIR) from just above 0.3 micrometers to 2.5 micrometers. It has 256 spatial pixels and will primarily be used in a pushbroom mode. Although it can operate at up to 240 Hz frame rate which makes an attractive cross track scanner, operation will primarily be between 15 Hz and 60 Hz to match the ground speed of the airborne platform, improve signal to noise and to limit the tremendous rate of data generation. TRWIS III features outstanding MTF, polarization insensitivity, spatial co-registration of spectral channels and cross track spectral performance. The data are quantized digitally at 12 bits and feature very high signal to noise ratio as illustrated in Figures 5 and 6. We are currently waiting for delivery of the two new custom focal planes. The focal plane to be used in the VNIR spectrometer is a four ported, split frame transfer CCD which is thinned and backside illuminated (for high quantum efficiency and to avoid the fringing associated

with the gate structure in front side devices). It has 768 spatial and 384 spectral detectors 20 micrometers square which are aggregated 3 by 3 to produce 256 spatial pixels and 128 spectral channels with 60 micrometer macro pixels. This CCD is limited to 1.2 million electrons in the summing well on readout which allows the VNIR assembly to be operated wide open, f/3.3, at 60 Hz for dark targets like the ocean. For targets which are significantly brighter or for slower frame rates the system would be stopped down to avoid saturation; improved MTF and spectral purity would result even though they are designed to be very good wide open. Figure 5 presents signal to noise ratio for a 5 percent albedo scene at 56 Hz, 10 nm spectral bandwidth and f/3.3. Also shown are curves for various scene albedos where the system is stopped down to prevent saturation at maximum brightness. As can be seen, very high signal to noise ratios are attained.

The SWIR focal plane is also a new development. It uses a 2.45 micrometer wavelength cut off Mercury Cadmium Telluride detector array based on the NICMOS technology which has 256 by 256 detectors each of which are 60 micrometers square. The 2.45 micrometer cut off reduces the thermal background as compared to detectors, such as InSb, whose responsivity extends much farther. This dramatically reduces noise and background drift with temperature. The readout/multiplexer is four ported and uses a capacitive-feedback transimpedance amplifier (CTIA) in each unit cell to provide the sensitivity and linearity at the low photon fluxes characteristic of imaging spectrometer operation. The integration capacitors are selectable, large or small, for different applications. The SWIR signal to noise ratios presented in Figure 6 are for 56 Hz and 12.5 nm spectral bandwidth. The very high signal to noise ratios are the result of long integration time characteristic of pushbroom operation, fast optics, low noise readout and especially low thermal background noise due to the 2.45 micrometer cutoff wavelength. A custom dewar has been designed to be compatible with the TRWIS III optical train. A commercial cryocooler will be used to cool the array to 115 k for low noise operation. We are scheduled to make data flights with TRWIS III in October of this year (1995) to support the SSTI Program. TRWIS III will be available after then to take data for other customers.

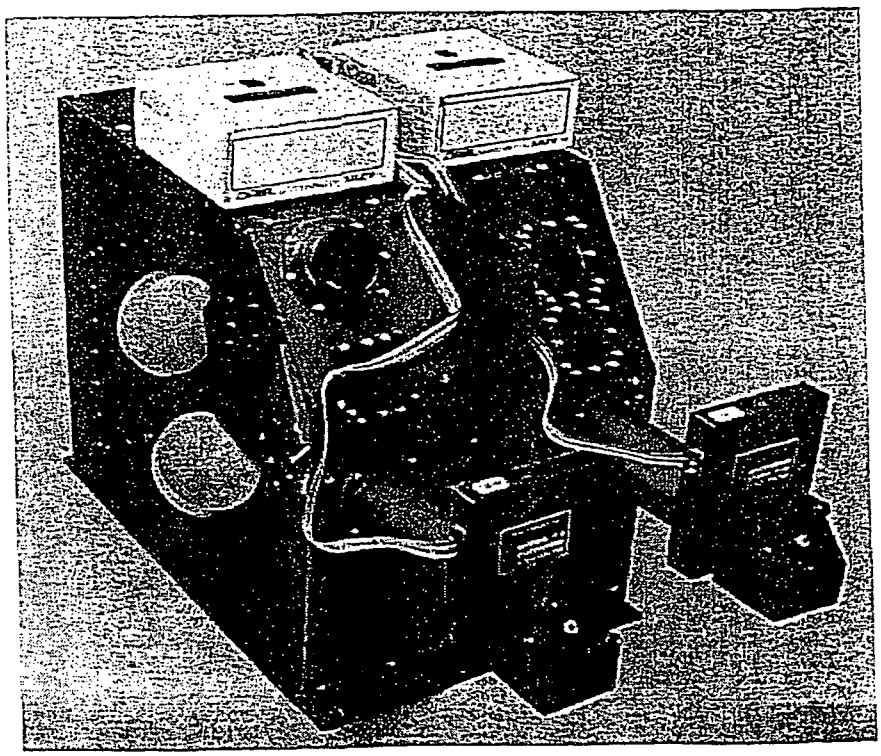

Figure 4 - TRWIS III

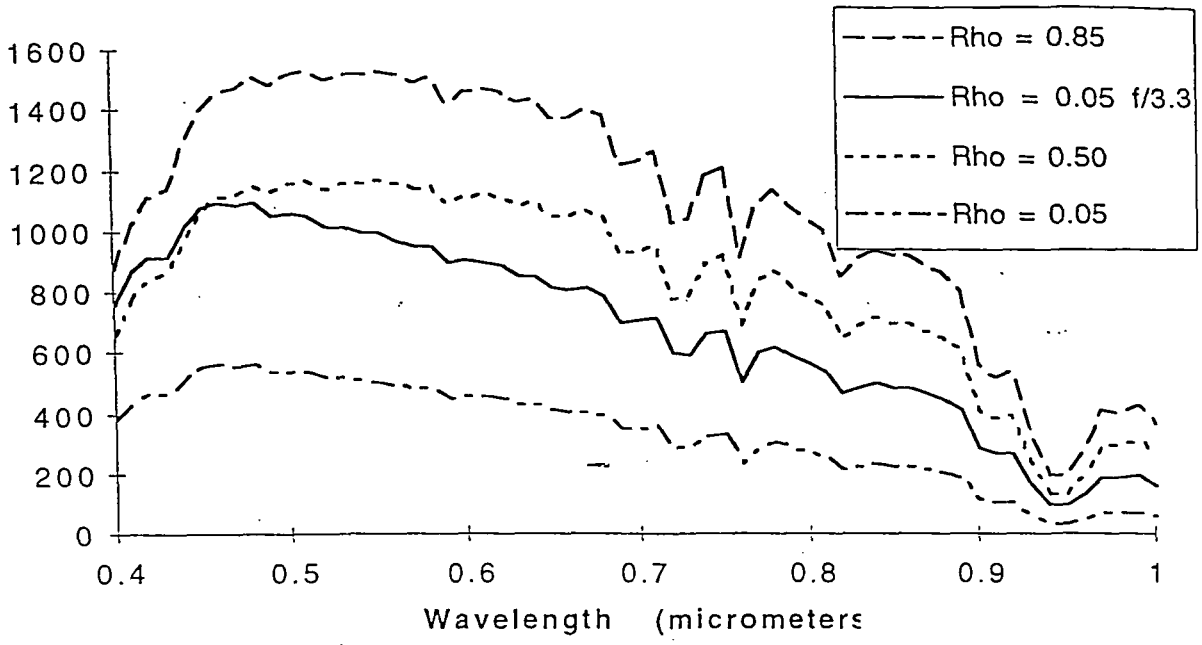

Figure 5 - TRWIS III VNIR Signal to Noise Ratio

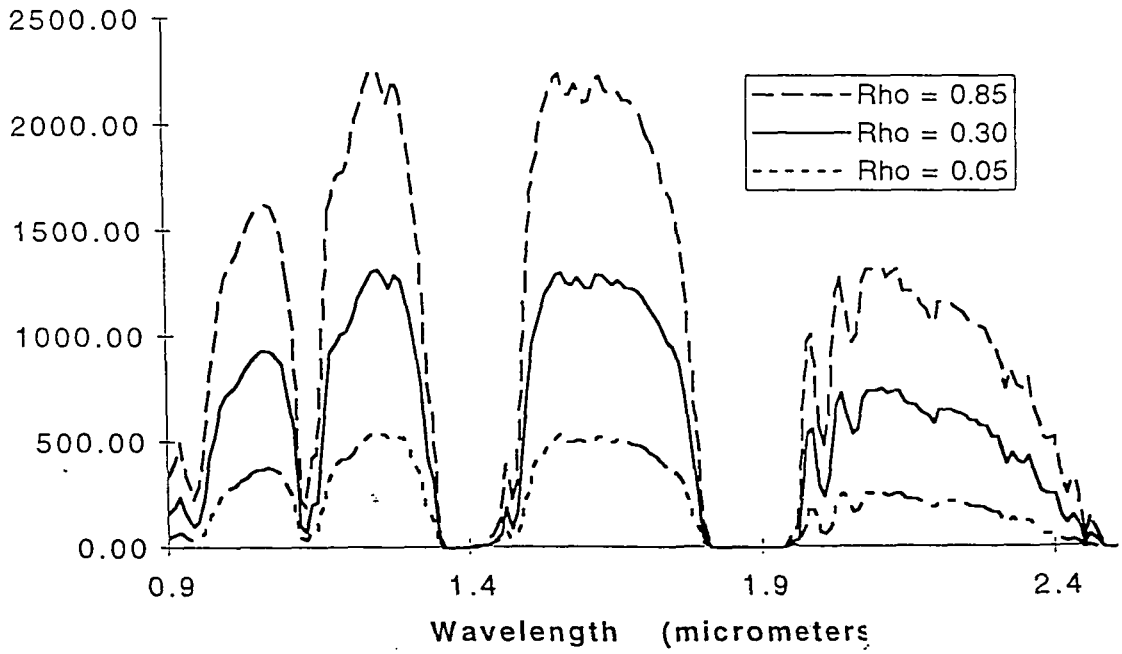

Figure 6 - TRWIS III SWIR Signal to Noise Ratio

SSTI HSI

The development of TRWIS III led to our design concept for the Hyperspectral Imager (HSI) as part of NASA's Small Satellite Technology Initiative. We began SSTI in July of

1994 and are in an 18 month development cycle to deliver the instrument next January (1996). The HSI, shown in Figures 7 & 8, provides a small, low cost system for space based hyperspectral remote sensing. The HSI Sensor Assembly envelope is roughly 17" wide by 22 " high by 31" long and weighs 23 kg. The HSI Control Electronics and HSI Power Electronics are shown to scale and add another 8 kg. The total orbit average power is 50 watts. HSI will use flight versions of the TRWIS III focal planes with entirely different optics to accommodate it's 523 km altitude. The optical design utilizes shared foreoptics to generate three line images separated slightly in field. The pixel size on the ground for the hyperspectral channels is 30 meters, the same as Landsat; and, a 256 pixel pushbroom swath covers 7.68 km. HSI is pointed by the spacecraft, with cross track pointing provided up to 20 degrees off nadir. Like TRWIS III, HSI has 384 spectral channels, which can be selected in any combination. The spectral range is from 0.4 micrometers to 2.5 micrometers; the two spectrometers overlap from 0.9 micrometers to 1.0 micrometers.

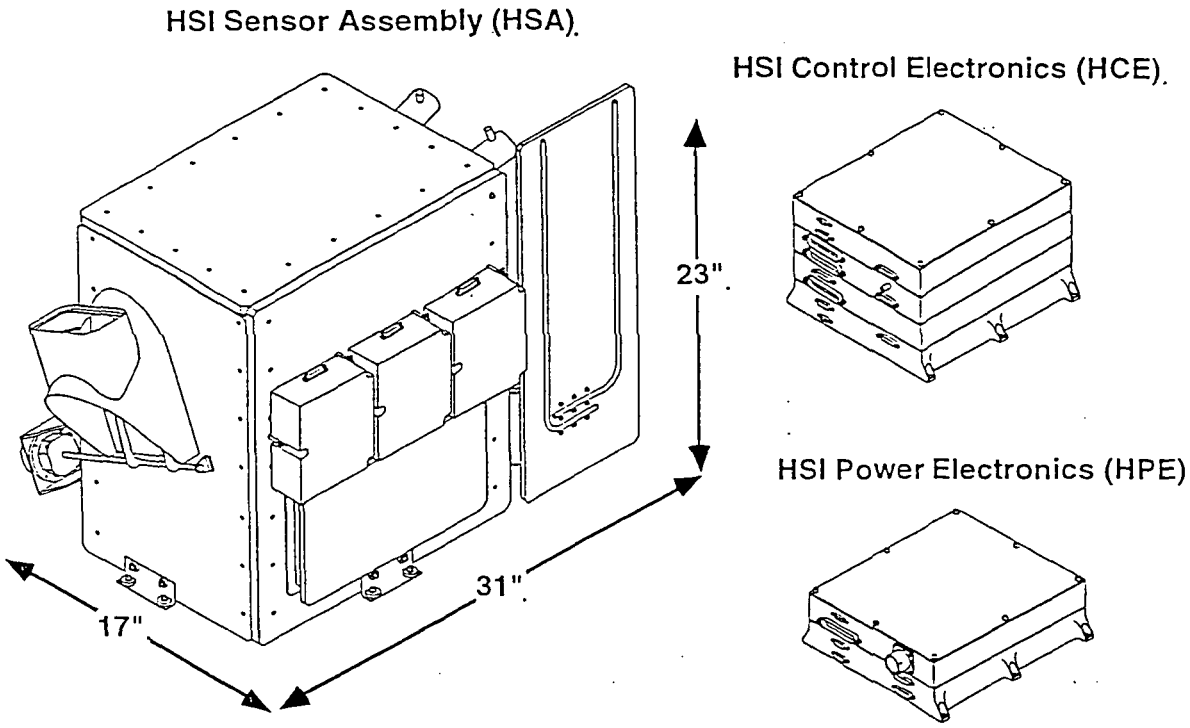

Figure 7 - SSTI Hyperspectral Imager Assemblies

HSI also has a single panchromatic visible channel (0.48 micrometers to 0.75 micrometers) which has 5 meter ground pixels in a swath of 2592 pixels or about 13 km wide. The panchromatic band allows for additional spatial sharpening of the 30 meter hypersectral images during ground processing. The instrument uses both solar and in-flight calibration sources for absolute radiometric accuracy of better than 6%. HSI uses a TRW miniature pulse tube cryocooler to cool the HCT focal plane to 115 k. The CCD focal planes are

cooled slightly, to 273 k, to reduce dark current noise. The instrument is partially redundant to achieve a five year design life. Data storage is provided by a solid state recorder in the spacecraft.

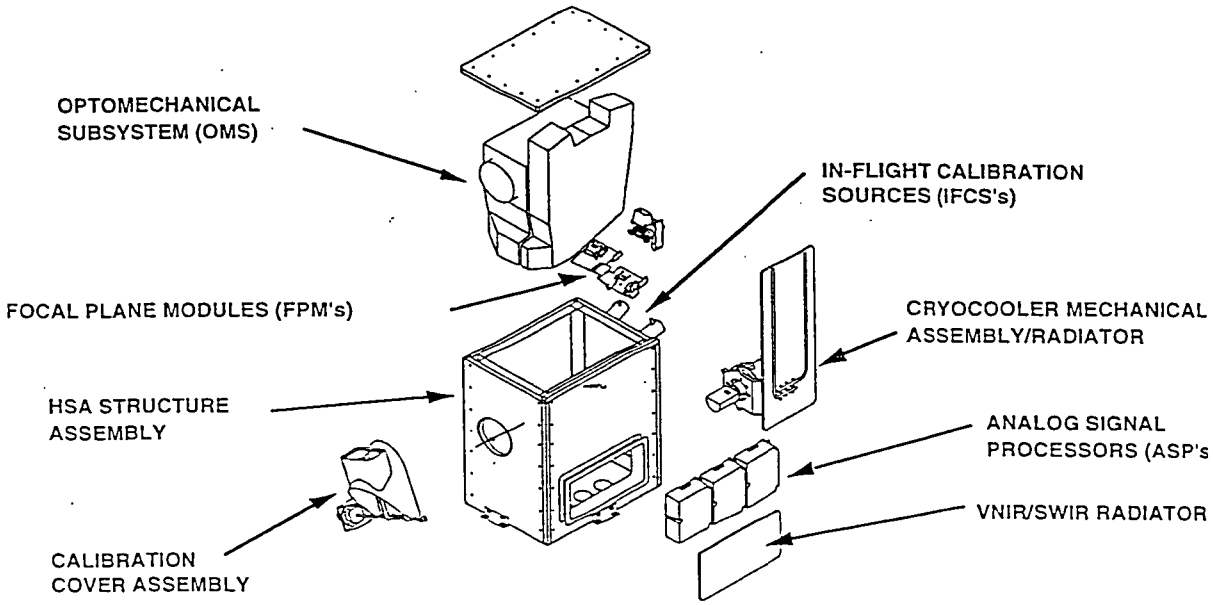

Figure 8 - SSTI Hyperspectral Imager Exploded View

Low Resolution Camera

The last instrument to be described here is an ocean color imager which we are developing for space flight. It is known as the Low Resolution Camera (LRC) since it has a pixel size of 850 meters at nadir and 1000 meters at the end of the 800 km swath from a 685 km altitude. It is a unique instrument because it generates its bands using a grating spectrometer rather than more conventional interference filters. The performance characteristics are presented in Table 2. The minimum resolution available is 10 nm with the band edges being placed anywhere within the total spectral capability to a tolerance of 2 nm. Broader bands are created by aggregating spectral coverage on the CCD for dim scenes or digitally for bright scenes. Although the instrument will be used for only six bands at a time they can be chosen over the whole 0.4 to 1.0 micrometer range. This allows the instrument operation to be optimized on-orbit for ocean or land applications. More bands could be digitized if they could be supported by onboard storage and down link capacity.

The instruments above were primarily pushbroom instruments. The LRC is a cross track scanner. It scans a 64 pixel image across the ground track in about seven seconds and retraces without imaging in about one tenth of that. It can look at a black target every scan to measure zero offset and has a white solar reflector which it can look at every orbit for gain calibration which results in a projected radiometric accuracy of better than 5 percent absolute. Figure 9 presents the LRC concept. The LRC is projected to weigh less than 6 kg, use less than 20 watts power in operation and less than 8 watts orbital average. It benefits from the development of HSI, TRWIS III and our other space instrument programs in the focal plane, spectrometer, thermo-mechanical design and electronics areas. No redundancy is required to meet the reliability requirement (i.e., > 0.90 at two years) due to its simple design. It affords an extremely low cost solution to this important

measurement need due to the simplicity of the concept and especially to the heritage of the focal plane and electronics.

Table 2 - Low Resolution Camera Performance Characteristics

Band Number	1	2	3	4	5	6
Band Center (nm)	443	490	510	555	670	865
Center Accuracy (nm)	< 2	< 2	< 2	< 2	< 2	< 4
Bandwidth (nm)	20	20	20	20	20	40
Width Accuracy (nm)	< 2	< 2	< 2	< 2	< 2	< 4
MTF	> 0.38	> 0.36	> 0.36	> 0.36	> 0.36	> 0.36
Design Radiance (watts/m^2-micron-ster)	84.1	65.6	56.4	45.7	24.6	10.9
SNR @ Design Radiance	814	932	902	883	694	546

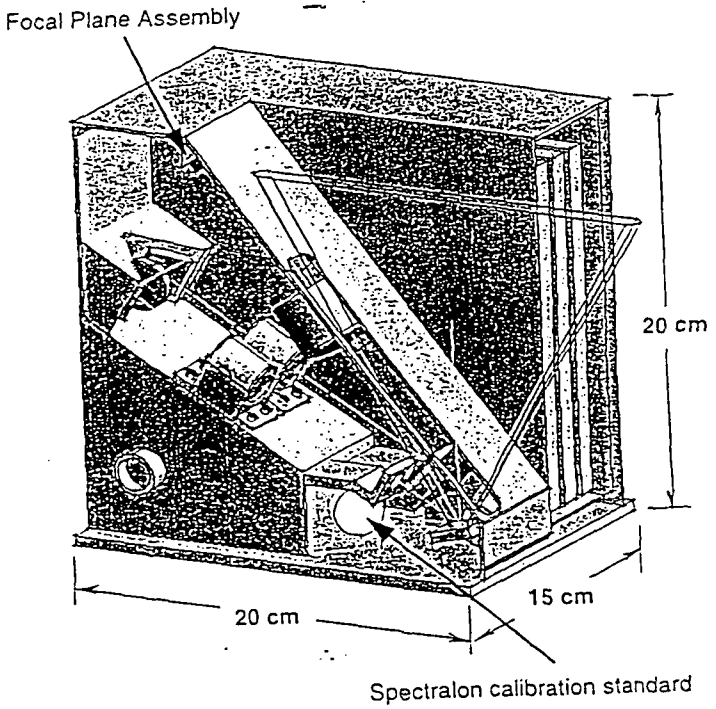

Figure 9 - Low Resolution Camera (Ocean Color Imager)

SUMMARY

TRW has been the hyperspectral imager business for more than five years and in the space instrument business for almost three decades. One of our current focuses is hyperspectral imaging which we have applied to several state of the art instruments. TRWIS III is designed be the highest performing aircraft instrument available when it comes on-line later this year. SSTI/HSI will be the first hyperspectral imager in space when it is launched in mid 1996. The LRC represents a new approach to applying existing technology cost effectively to an old problem while yielding exceptional performance and flexibility. TRW has made significant capital investments in hyperspectral related technologies over the last several years and is committed to the growth and development of this exciting new technology.

Appendix 2 - UCB

N15

An Instrument to Study the Diffuse EUV Astronomical Background

S. BOWYER,[1] J. EDELSTEIN,[1] M. LAMPTON,[1] L. MORALES,[2]
J. PEREZ MERCADER,[3] AND A. GIMENEZ[3]

[1] Center for EUV Astrophysics, 2150 Kittredge St.,
University of California, Berkeley, CA 94720-5030, USA
[2] Universidad Autonoma de Madrid, Ciudad Universitaria de Cantoblanco,
28049 Madrid, Spain
[3] LAEFF, Instituto Nacional De Tecnica Aerospacial,
Apartado de Correos 50727, 28080 Madrid, Spain

The extreme ultraviolet (EUV) diffuse background is the most poorly known of any of the diffuse astronomical backgrounds. Only upper limits to this flux exist, obtained with spectrometers with very crude (from $\approx$ 15 to 30 Å) resolution; these limits are generally one to two orders of magnitude larger than the expected sources of cosmic flux. A variety of source mechanisms have been postulated to radiate in this bandpass; the most discussed is the hot phase of the interstellar medium. A speculative possibility is that hot dark matter in the form of massive, radiatively unstable neutrinos in our Galaxy will produce a unique line in this bandpass. We describe an instrument employing a new type of spectrometer which will provide ~5 Å resolution and unprecedented sensitivity for diffuse EUV radiation. The instrument will be carried aboard the newly developed Spanish Minisat satellite.

1. Introduction

Initial investigations of the diffuse astronomical background in the EUV were carried out with broad-band detectors on rockets and short duration orbital flights (Cash, Malina, & Stern 1976; Stern & Bowyer 1979; Bloch et al. 1986). The *Alexis* Satellite developed by the Los Alamos group was designed to provide broad band measurements of the cosmic EUV flux (Bloch et al.); and Lieu et al. (1995) obtained upper limits to this flux with EUVE.

A few spectrographic measurements have been made. Holberg (1986) obtained data from 520 to 1100 Å with 30 Å resolution with the Voyager 2 ultraviolet spectrometer. Edelstein & Bowyer (1995) have noted that the Voyager upper limits were overly stringent and have derived more appropriate limits from this data. Labov & Bowyer (1991) flew a grazing incidence spectrometer to measure the cosmic background from 80 to 650 Å with a resolution of 15 Å on a sounding rocket. These authors tentatively identified features which might have been produced by the hot phase of the ISM, but the features noted were close to the limiting sensitivity of the instrument and are now believed to be spurious (Edelstein & Bowyer 1995). Jelinsky et al. (1995) made innovative use of the spectrometers on *EUVE* to obtain astronomically important upper limits to the EUV background. The Wisconsin group has developed an instrument to carry out soft X-ray spectroscopy on the diffuse cosmic background; preliminary results from this experiment are presented elsewhere in this Volume.

2. Diffuse Cosmic Emission Mechanisms

It has been more than thirty years since Spitzer (1956) suggested that hot, million-degree gas pervades our Galaxy and more than twenty years since the soft X-ray background (now generally believed to be produced by a high-temperature component of the

ISM) was first detected (Bowyer, Field, & Mack 1968). However, models ascribing this emission to a high temperature plasma have been surprisingly unsuccessful (Cox 1995). If the diffuse soft X-ray background is the product of emission from a hot gas, much of the radiated power will be in emission lines from highly ionized atoms radiating at EUV wavelengths.

The actual lines observed from a hot ISM will be strongly dependent upon the temperature and thermal history of this material (Breitschwerdt & Schmutzler 1994). Several temperatures have been suggested for this phase. Soft X-ray data suggest 10^6 K gas (Cox & Reynolds 1987). Absorption line data showing O VI (Jenkins 1978a,b) is often cited in combination with the soft X-ray data as further evidence for a 10^6 K gas, but the peak of the emission curve for O VI is at the substantially lower temperature of $\sim 3 \times 10^5$ K. High ionization absorption lines observed in stellar spectra taken with *IUE* indicate a temperature of 3×10^5 K (Savage 1987) as does the observation of emission lines at far UV wavelengths (Martin & Bowyer 1989). Breitschwerdt & Schmutzler (1995) have suggested that the soft X-ray emission is the product of residual high ionization states and that the actual kinetic temperature of this plasma could be as low as 4×10^4 K.

A speculative possible contributor to the cosmic EUV background is emission from neutrinos in our Galaxy undergoing radiative decay. This scenario has been explored in substantial detail in a series of papers by Sciama and co-workers (Sciama 1994). Evidence for this emission has been searched for but not found in *IUE* data taken on a quasi-stellar object which lies in a cluster of galaxies (Fabian, Naylor, & Sciama 1991), and with the Hopkins Ultraviolet Telescope, which observed a cluster of galaxies on the flight of ASTRO I (Davidsen et al. 1991). In both cases the line would have been sufficiently redshifted to move it into the bandpass observed. Though these results have been generally interpreted as ruling out the Sciama hypothesis, Bowyer et al. (1995) have shown that this is not correct and that Sciama's hypothesis is still viable.

3. The Instrument

We have developed an instrument to measure the diffuse EUV background. We have employed normal incidence rather than grazing incidence optics in this instrument because this allows a folded light path and a much smaller instrument size. Through the use of special coatings, this instrument reaches wavelengths as short as 350 Å.

A spectrometer for diffuse radiation disperses radiation viewed through an aperture to a single location on the detector corresponding to the wavelength of the radiation. The observed intensity depends on the product of the area of the aperture times the solid angle of the sky observed. Increasing the width of the aperture increases this product but will degrade the overall spectral resolution. Increasing the solid angle by increasing the aperture height will also increase this product, but grating aberrations in existing spectrograph designs increase rapidly for off-axis rays, strongly limiting the extent to which this parameter can be increased. For example, a conventional Rowland spectrometer performs well for point sources on axis, but has severe aberrations for radiation as little as 1° off-axis.

To determine potential combinations of grating surface and ruling parameters for an optimum diffuse radiation spectrometer, we developed a general expression describing the optical path for radiation incident upon an arbitrary polynomial surface with variable space diffraction rulings converging to a single point on the detector. We chose plane-cylindrical radiation eminating from a slit aperture as a source. In contrast, the Rowland spectrograph utilizes a spherical source from a point on the slit. Following Fermat's Principle, we minimized variation of the path function over the grating's aperture and found solutions which eliminated aberrations to third order for on-axis illumination and

FIGURE 1. Schematic diagram of the optical design of the spectrometer.

retained most of this performance well off-axis. Constant line spacing and rotationally symmetric grating surfaces were then imposed on our solution to simplify the ruling and figuring process, and approximations to the optimum theoretical solution were sought. An elliptical surface was found to provide a solution close to theoretical and this was numerically raytraced over a range of illumination angles and wavelengths to verify the predicted parameters. This design retained at least 80% of its performance to 4° off axis. Moreover, spatial resolution better than 0.1° is achieved along the sky in the direction along the spectrograph slit, which permits radiation from bright stars to be identified and removed. A schematic of the optical design is shown in Figure 1.

A major innovation is the use of a low internal background multichannel plate detector used in connection with wedge and strip encoding (Lampton et al. 1986). At EUV wavelengths a prime contributor to the noise is background in the detector (Lieu et al. 1993). This background consists of two components (a) an internal background due to the radioactive decay of potassium in the microchannel plates, and (b) a charged particle background. We employ special microchannel array plates with no potassium and surround the detector with a charged particle anticoincidence system to significantly reduce both of these backgrounds.

Two of these spectrometers will be flown as a single instrument package (the Espectrografo Ultravioleta extremo para la observacion de la Radiacion Diffusa, or EURD) on the Spanish Minisat satellite in 1996. The gratings on these spectrographs have different

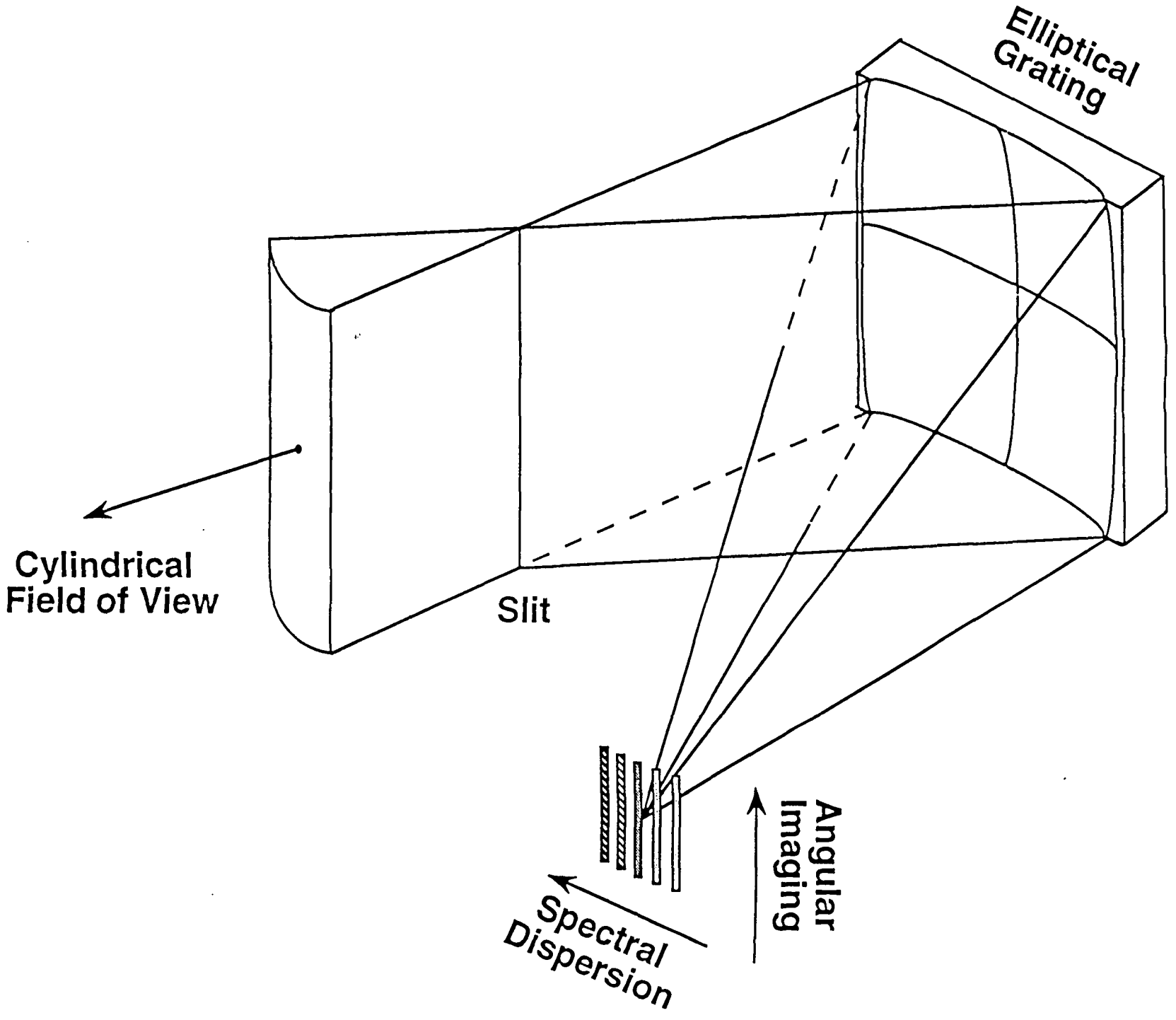
Elliptical
Grating
Cylindrical
Field of View
Slit
Angular
Imaging
Spectral
Dispersion

TABLE 1. Key Instrument Parameters

Bandpass:	350–1100 Å
Field of view:	26° × 8°
Grating:	8 cm diameter 18 cm focal length holographically ruled 2460 lines mm^{-1}
Grating overcoating:	long wavelength: silicon carbide short wavelength: boron carbide
Detector:	Multichannel plate with wedge and strip encoding
Detector photocathode:	magnesium fluoride
Size (each spectrograph):	40 × 40 × 13 cm
Weight (each spectrograph):	11 kg

coating to optimize the shorter and longer bandpasses of the total bandpass covered. A summary of key instrument parameters is provided in Table 1.

4. Flight Electronics and Software

The first stage detector electronics consists of three ultra low noise charge sensitive amplifiers which receive the microchannel plate signals and provide shaped pulse signals to the downstream analog-to-digital conversion system. These charge amplifiers are especially designed to be free of overload saturation artifacts from cosmic-ray events, and are designed to provide image stability over the three year duration of the mission.

An important part of the detector electronics is an electronic pulse calibration system. Each second, a trio of charge pulses is generated by an onboard quartz-crystal controlled oscillator. The amplitudes of these pulses are controlled by a digitally switched attenuator to produce accurate charge signals for the detector electrodes; these charge amplitude ratios have been chosen to encode positions in the extreme corners of the field of view of each detector. In this way, the stability of the entire detector electronics can be monitored through instrument development, calibration, test, integration, and during the mission.

The digital flight electronics system is centered in a high capability microprocessor with associated ROM, RAM, control logic, and communications chips. The architecture adopted is based on the flight proven ATT DSP32C microprocessor. Although this chip family is radiation tolerant, specific provisions have been taken to assure its survival in case of latchup triggered by a high energy cosmic ray event.

There are two principal functions of the EURD microprocessor. A photon formatting task takes random photoevents in their wedge-strip format and converts them into event (x,y) coordinates using full 32-bit arithmetic in order to avoid introducing computational artifacts into the accumulated images. Each event is flagged with the anticoincidence shield status along with a variety of other information.

The data communications task of the EURD microprocessor executes concurrently with the photon formatting. Data are transferred to and from the spacecraft bus in a high-speed block format. The EURD processor is continuously available to receive a command block, or to dispatch a data block to the onboard data storage system.

5. Overall Performance

In Figure 2 we compare the predicted sensitivity for the EURD spectrometers for 100 hrs and 1000 hrs of observing time with the best upper limits available in the bandpass

TABLE 2. Diffuse Galactic ISM Experiments

	Bandpass	Resolution (E/ΔE)
EUVE (Jelinsky et al. 1995)	190–250 Å	10
	400–460 Å	10
Los Alamos (Bloch et al., 1995)	130–190 Å	10
Wisconsin (Sanders et al., 1995)	40–80 Å	20
Penn State (Burrows et al. 1995)	10–50 Å	40–60
This experiment	350–1000 Å	200

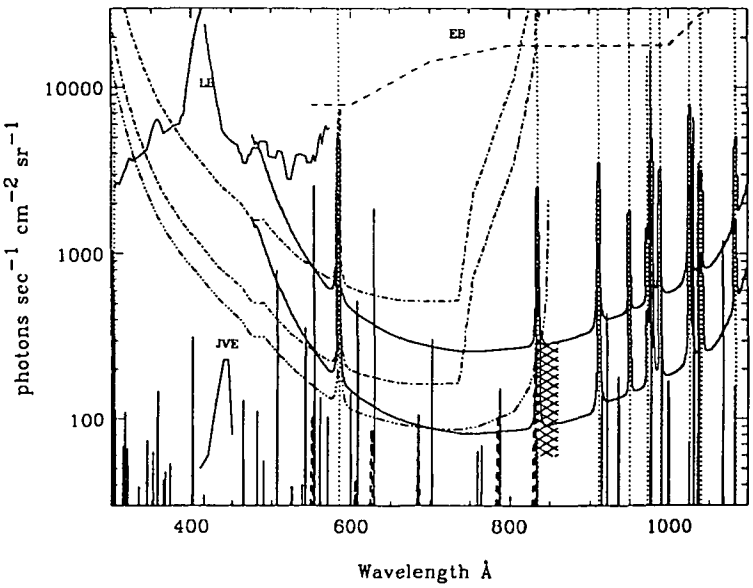

FIGURE 2. Existing upper limits to the diffuse EUV cosmic background. LB are the 15 Å resolution limits of Labov and Bowyer. EB are the 30 Å resolution limits derived by Edelstein and Bowyer from Voyager data. JVE are the limits of Jelinsky et al. The curved, solid, horizontal lines are the flux limits provided by 100 and 1000 hrs of observation with the long wavelength spectrometer. The curved, dot-dashed, hotizontal lines are the same limits for the short wavelength spectrometer with the aluminum filter. The lower dash-triple dot line show similar limits with no filter. The solid vertical lines are the expected ISM emission from a steady-state collisionally ionized plasma. The heavy dashed vertical lines are the intensities from the delayed recombination model of Breitschwerdt and Schmutzler. The dotted vertical lines are expected airglow lines. The cross-hatched region shows the range of the emission predicted by Sciama for a halo of radiatively decaying neutrinos.

covered. Two distinct models of interstellar line emission are also shown. One model assumes collisional ionization equilibrium, using the emissivities of Monsignori-Fossi & Landini (1995) and the emission measure from Bowyer et al. (1995). The other model is the delayed recombination model of Breitschwerdt & Schmutzler (1994 and private communication) whose intensity fits the 0.25 keV soft X-ray background at high galactic latitudes and for which we have assumed attenuation due to the ISM in local cloud of 5×10^{17} (Frisch 1994). The line from decaying neutrinos is from Sciama (1994), and the airglow lines are from Chakrabarti et al. (1984).

In Table 2, we summarize key parameters of instruments which have been, or will soon be used to study the character of the diffuse EUV and soft X-ray background. The EURD instrument has substantial capabilities both in absolute terms and in comparison with these other instruments.

We thank Eric Korpela for help in various aspects of this development and for useful discussions. Gerald Penegor, Josef Dalcolmo, Charles Donnelly, and Ray Chung provided important technical contributions. This work was supported by NASA Grant NRG05-003-450.

REFERENCES

BOWYER, S., FIELD, G., & MACK, J. 1968, Nature, 217, 32

BOWYER, S., LIEU, R., SIDHER, S. D., LAMPTON, M., & KNUDE, J. 1995, Nature, 375, 212

BLOCH, J. J., JAHODA, K., JUDA, M., MCCAMMON, D., SANDERS, W. T., & SNOWDEN, S. L. 1986, ApJ, L, 308, L59

BLOCH, J. J. 1995, This volume

BREITSCHWERDT, D. & SCHMUTZLER, T. 1994, Nature, 371, 774

BREITSCHWERDT, D. & SCHMUTZLER, T. 1995, IAU Symposium 171: New Light on Galaxy Evolution, Heidelberg 1995, Kluwer Academic Publishers, Ralf Bender & Roger Davies, eds

BURROWS, ET AL. 1995, submitted to the SPIE Proceedings Volume 2518: EUV, X-Ray & Gamma-Ray Instrumentation for Astronomy VI

CASH, W., MALINA, R., & STERN, R. 1976, ApJ, L, 204, L7

CHAKRABARTI, S., KIMBLE, R., & BOWYER, S. 1984, J. Geophys. Res., 89, 5660

COX, D. P. & REYNOLDS, R. J., 1987, Ann. Rev. Astron. & Astrophys., 25, 303

COX, D. P. 1995, This volume

DAVIDSEN, A., ET AL. 1991, Nature, 351, 128

EDELSTEIN, J. & BOWYER, S. 1995, ApJ, submitted

FABIAN, A. C., NAYLOR, T., & SCIAMA, D. W. 1991, Mon. Not. R. Astron. Soc., 249, 21

FRISCH, P. 1994, Science, 265, 1423

HOLBERG, J. B. 1986, ApJ, 311, 969

JELINSKY, P., VALLERGA, J. V., & EDELSTEIN, J. 1995, ApJ, 442, 653

JENKINS, E. B. 1978a, ApJ, 219, 845

JENKINS, E. B. 1978b, ApJ, 220, 107

LABOV, S. E. & BOWYER, S. 1991, ApJ, 371, 810

LAMPTON, M., SIEGMUND, O. H. W., BIXLER, J., & BOWYER, S. 1986, SPIE Tucson, 627, 47

LIEU, R., BOWYER, S., LAMPTON, M., JELINSKY, P., & EDELSTEIN, J. 1993, ApJ, 417, L41

MARTIN, C. & BOWYER, S. 1989, ApJ, 338, 677

MONSIGNORI-FOSSI, B. & LANDINI, M. 1995, This volume

SANDERS, W. T. & EDGAR, R. J. 1995, This volume

SAVAGE, B. D. 1987, in Interstellar Processes, ed. Hollenbach & Thronson, D. Reidel Publishing, Dordrecht, Netherlands

SCIAMA, D. W. 1994, Modern Cosmology and the Dark Matter Problem, Cambridge University Press, New York

SPITZER, L., JR. 1956, ApJ, 124, 20

STERN, R. & BOWYER, S. 1979, ApJ, 230, 755

Appendix 3 - PRKE

95N 17276

AIAA-95-0030

A Modular Electric Power System Test Bed for Small Spacecraft

R.M. Button and A.N. Baez
NASA Lewis Research Center
Cleveland, OH

33rd Aerospace Sciences Meeting and Exhibit
January 9–12, 1995 / Reno, NV

A MODULAR ELECTRIC POWER SYSTEM TEST BED FOR SMALL SPACECRAFT

Robert M. Button
Anastacio N. Baez
National Aeronautics and Space Administration
Lewis Research Center
Cleveland, OH 44135

ABSTRACT

In the new climate of smaller, faster, and cheaper space science satellites, a new power system topology has been developed at the NASA Lewis Research Center. This new topology is based on a series connected boost converter (SCBC) and can greatly affect the size, weight, fault tolerance, and cost of any small spacecraft using photovoltaic solar arrays. The paper presents electric power system design factors and requirements as background information. The series connected boost converter topology is discussed and several advantages over existing technologies are illustrated. Besides being small, lightweight, and efficient, this topology has the added benefit of inherent fault tolerance. A positive ground power system test bed has been developed for the TROPIX spacecraft program. Performance of the SCBC in the test bed is described in detail. SCBC efficiencies of 95% to 98% have been measured. Finally, a modular, photovoltaic regulator "kit" concept is presented. Two (2) SCBCs are used to regulate solar array charging of batteries and to provide "utility-type" power to the user loads. The kit's modularity will allow a spacecraft electric power system to be built from off-the-shelf hardware; resulting in smaller, faster, and cheaper spacecraft.

INTRODUCTION

The recent failures of several large spacecraft have led NASA to rethink its policy towards space science missions. The initial problems with the Hubble Space Telescope and the loss of the Mars Observer have drawn much public attention—their big price tags and long development times have put them under the scrutiny of Congress and the public. Although space science is difficult and risky, new and better ways to achieve our nation's goals in space need to be addressed. Small, low cost spacecraft that can be developed in less than 3 years are being considered as the wave of the future in space science.

Many of these small spacecraft will have missions in and around Earth orbit. The low Earth orbit (LEO) is characterized by constant and frequent eclipses of the sun requiring high quality and long life batteries. Power requirements in the 1kW-5kW range will be typical. Solar arrays and flight rated batteries will be the typical source of electrical energy.

These similarities in the power system requirements can lead directly to similar power systems. However, it is still common for a new spacecraft to completely develop a power system from the ground up. The cost of custom made space electronics is extremely high and accounts for a major portion of the spacecraft power system development cost. Today's commercial electronic parts are extremely reliable and can possibly be used in spacecraft power systems to reduce costs. Also, by modularizing key power system components, much time, manpower, and money can be saved by allowing spacecraft designers to "build" their power system with off-the-shelf components designed to work together. This building block approach results in inexpensive spacecraft and short development times.

NASA Lewis Research Center has established the necessary groundwork and expertise in power systems and controls to investigate advanced modular electric power system (EPS) architectural concepts for small spacecraft. A small test bed based on a modular power system concept has been developed using the Electric Power System Test Bed in the Power Systems Facility at NASA Lewis. This world-class test facility was developed in support of the independent evaluation of the Space Station power system design.[1]

EPS DESIGN FACTORS

In a photovoltaic power system, several unique characteristics of the energy source and storage systems must be accounted for in the system design. These characteristics usually result in system requirements which address problem areas and make the most efficient use of the energy generated. Some examples are requirements for a fault tolerant power system and use of a "utility-type" power distribution. These requirements will greatly affect both the component and overall system design.

Photovoltaic Arrays

Since the 1960's solar cell arrays have been the choice for power generation in space. Their low mass, relatively long life, and ease of construction make them attractive electrical power sources. However, disadvantages include a low efficiency (typically below 17%), large surface area, complex deployment mechanisms, and degradation over time.

Solar arrays have unique power generation characteristics which present challenges to the EPS design. They are characterized by a well known current vs. voltage (I-V) curve which is directly related to the solar cells' diode-like construction. Figure 1 shows a typical I-V curve and its corresponding P-V curve (power vs. voltage). The I-V curve is defined by —

I_{sc} - the short circuit current

V_{oc} - open circuit voltage

V_{mp} - maximum power point voltage

These characteristics are largely determined in the construction of the array by wiring the individual solar cells in series and parallel combinations. However, these cell characteristics can vary over time and affect the power generation capability of the array.

Short circuit current is dependent on the insolation which strikes the cells. This can be reduced due to degradation of the protective covering, contamination, or by simply moving farther away from the sun. The solar array open circuit voltage is a function of array temperature. Cold arrays emerging from eclipse have a period of high V_{oc} until the array heats up to its nominal temperature. The maximum power point is a function of all the above—it moves with both Isc and V_{oc}.

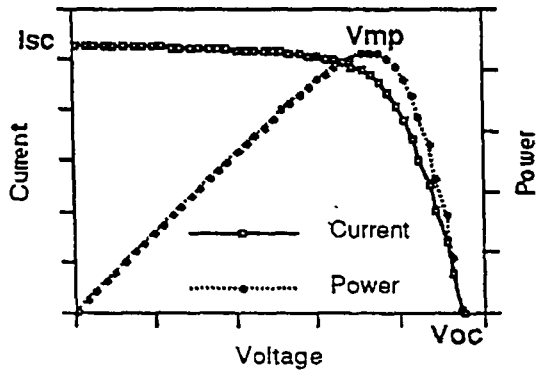

Figure 1 — Solar Array I-V Curve

In sizing solar arrays for spacecraft missions the EPS designer must take these factors into account. The array must be sized so that its end-of-life (EOL) power is sufficient to meet spacecraft power demands. Components must also be able to handle the high voltages generated as cold arrays emerge from eclipse.

Battery Charge Management

Battery technology has been challenged by modern spacecraft which are smaller, lighter, and required to operate over longer periods of time. Especially challenging is the operation in low Earth orbit (LEO) which is characterized by frequent charge-discharge cycles and long eclipse times of up to 30% of the orbit. By increasing depth of discharge (DOD), the battery size and weight can be reduced while still providing the energy storage needed. However, increased DOD reduces the battery operating life. This poses problems to EPS designers who are forced to balance battery DOD with long operating lives.

Battery lifetime and energy density can be maximized using established charge management guidelines. Controlling the charge current during insolation can have a great impact on battery life span and size. Charge management can prevent overheating of the cells and extend the lifetime of the battery. Also, the use of taper and trickle charge cycles can extend battery lifetimes. It's clear that careful charge management is necessary to optimize use of spacecraft batteries.

Fault Tolerance

Past charge management designs have relied on power converters between an unregulated solar

array bus and the battery. These designs work well and can be efficient, but, the entire battery can be lost if the power converter fails.

The recent failure of the NOAA-13 meteorological satellite was attributed to a short circuit in the battery charger electronics which prevented the solar arrays from charging the batteries. A fault tolerant power topology would have isolated the fault and allowed the arrays to directly charge the batteries. Losing the battery charge management would have reduced the operating life of the spacecraft. However, the solar arrays could have charged the batteries and operated normally for some time.

Other designs have used bidirectional DC-DC converters to charge the batteries during insolation and to provide regulated voltage during eclipse. These converters tend to be large, inefficient, and subject to a single fault which will fail the energy storage system of the entire power channel.

Yet other methods have controlled the solar array output through highly efficient converters. The output of the array is varied to affect the charge current into the battery. Similar to the methods above, failure of the array regulator will disable the entire power channel.

User Power Regulation

In some power systems, the users' (experiments, instruments, and spacecraft loads) are connected directly to the battery bus. In most cases these loads require DC-DC converters to convert the unregulated bus to usable voltage levels (typically 5 and ±12 Vdc). These load converters must handle large voltage swings since the battery bus voltage can vary by up to 25% through the full range of charge and discharge cycles. These converters tend to be larger and less efficient than a converter which is designed for a specific input voltage level.

A "utility-type" power system delivers power to the users at a tightly regulated voltage. To accomplish this, the spacecraft EPS must provide regulation during insolation and eclipse periods, usually by means of a DC-DC converter. The converter is the interface between the primary, or source, bus and the secondary bus. By providing a regulated voltage to the user loads their DC-DC converter designs can be optimized for a specific input voltage. The smaller, more efficient converters will have a positive impact on the overall spacecraft size and weight.

SERIES CONNECTED BOOST CONVERTER

A new power converter interconnection technology has been developed at the NASA Lewis Research Center which is ideally suited for photovoltaic power systems. The converter is called a series connected boost converter (SCBC) and provides size, weight, efficiency, and fault tolerance benefits over existing technologies.[2]

The SCBC is based on an isolated, step-down DC-DC converter. A block diagram of the SCBC is shown in Figure 2. Because the converters' output is isolated from the input it can be connected such that the output is in series with the input. By referencing the output voltage to the input return line, the resulting output voltage is "boosted" from the input voltage by the converter. However, the converter only processes a fraction of the total power delivered. The amount is determined by the ratio of boost voltage to output voltage. The majority of the current simply bypasses the DC-DC converter, passing through the transformer secondary windings and the rectifier diodes.

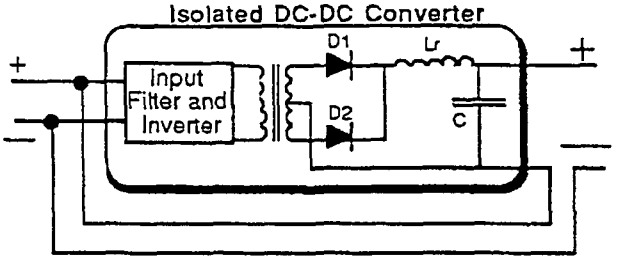

Figure 2 — Series Connected Boost Converter

Power Density and Efficiency

The series connected boost connection allows a converter to control more than its rated power level. In the SCBC, the DC-DC converter processes only a fraction of the total power delivered; most of the power is bypassed through the series connection. Consequently, the size and weight of the SCBCs are smaller than a similarly rated, conventional DC-DC converter.

The SCBC is very efficient since it only has to process a portion of the total power delivered. Any power that bypasses the converter

experiences only filter losses and diode conduction losses. Efficiencies in the lab have been measured between 95% and 98% using standard, isolating DC-DC converters which had individual efficiencies of 85% to 90%. An illustration of how the SCBC leverages power and improves efficiency is given below:

DC-DC Converter Specs. (225W)

Input = 21-56 Vdc
Output = 15 Vdc @ 225W
Efficiency = 90%

800 W SCBC (zero boost)

Input = 55 Vdc
Output = 55 Vdc @ 14.5 A
Diode losses = 14.5 A • 0.7 V = 10 W
Filter losses = 5 W
TOTAL Losses = 15 W = **98.13% efficient.**

800 W SCBC (15Vdc boost)

Input = 40 Vdc
Output = 55Vdc • 14.5 A
Converter = 15 Vdc • 14.5 A = 218 W
90% efficient = 22 W of converter losses
Add fixed losses = 15 W
TOTAL losses = 37 W = **95.38% efficient.**

Obviously the gains in efficiency depend upon the DC-DC converter efficiency, the amount of fixed losses, and the boost voltage to output voltage ratio.

Fault Tolerance

Perhaps the most significant advantage of the series connected boost converter over other power converters is its ability to mitigate a complete failure of the power electronics. In other converters, such as the buck regulator, a failure of the power electronics or control circuits will completely disable the power delivery of that converter. However, the SCBC's unique connection allows for power to bypass a failed converter through the transformer secondary windings and rectifier diodes. Even when the DC-DC converter in the SCBC fails, the "zero boost" power is still available at the output of the converter. This fault tolerance characteristic makes the SCBC an ideal interface between a solar array and a battery.

Solar Array to Battery Interface

The SCBC can be used to regulate the battery charge current by controlling its boost voltage. Even as the array characteristics change (I_{sc} and V_{oc}), the SCBC is able to control battery charge current while delivering full power to the system. However, it is important that the array and batteries be sized properly for the SCBC operation at the extreme conditions. At the beginning of life (BOL) the cold array will produce excess power. However, the battery charge current cannot exceed I_{sc} and the voltage will be clamped to the battery. At the end of life (EOL) the degraded array must operate at the peak power point to deliver sufficient power. The SCBC must be sized so that the array voltage at maximum power, V_{mp}, can be boosted to provide full battery charge current.

Commonality

Finally, the series connected boost converter makes an excellent "building block" for a photovoltaic power system. By using a voltage regulator circuit the SCBC can be used to deliver regulated battery voltage to the spacecraft loads. Similarly, a SCBC can control battery charge current by simply adding a current regulator circuit. The DC-DC converter can also be used in its native mode to isolate a sensitive load from the spacecraft power system. By using one common DC-DC converter as a building block for the entire electric power system both, development costs and flight hardware costs can be reduced.

TROPIX EPS TEST BED

The recent failure of the ANIK 2 satellite due to transient, high energy fields in the Earth's magnetosphere have led to a proposed science satellite named TROPIX (Transfer Orbit Plasma Interaction Experiment).[3] The main purpose of the TROPIX satellite is to fully map the Earth's magnetosphere and investigate—

Magnetic and Electric Fields,
Low energy plasma, and
Energetic particles.

By fully understanding the Earth's magnetosphere, spacecraft can be designed to withstand the high energy plasma fields and mitigate damage to the electric power system.

A secondary mission of the TROPIX spacecraft is to demonstrate the feasibility of solar electric propulsion. Low thrust solar electric propulsion (SEP) allows a slow, nearly circular orbit procession from low Earth orbit to beyond geosyncronous orbits. Accuracy of the magnetic and electric field measurements improve as the TROPIX spacecraft

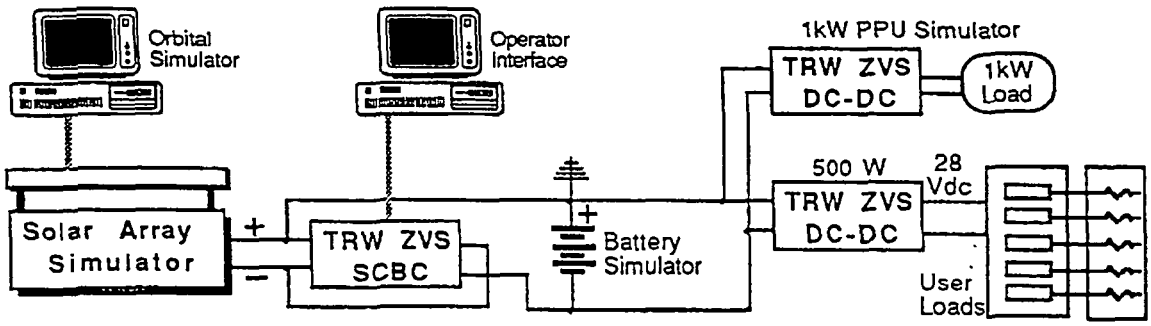

Figure 3 - TROPIX EPS Test Bed Block Diagram

slowly spirals through the magnetosphere.

The use of SEP for the TROPIX satellite places high importance on the electric power system. Power requirements include two (2) 900 Watt SEP engines and about 350 Watts of user loads (communications, navigation, and the science experiments) for a total power of 2.2 kW. The TROPIX satellite must also have a positive-ground power system due to the nature of the plasma science instruments. By positively grounding the solar arrays, interaction with plasma fields are greatly reduced.

An electric power system test bed was developed for the TROPIX program as a technology demonstrator of a positive-ground power system based on the SCBC.

Objectives

Objectives of the TROPIX EPS Test Bed were to provide an inexpensive test capability for the program and to demonstrate the power system technology necessary for solar electric propulsion. By providing a system test capability, the series connected boost converter topology in a positive ground configuration could be developed and evaluated. System level tests will provide data for power system sizing and control. In addition, data acquisition requirements could be defined. This Phase I test bed development effort was completed in seven months.

Test Bed Description

The TROPIX EPS Test Bed block diagram is shown in Figure 3. To reduce development costs, the test bed was constructed using power supplies, bulk DC-DC converters, and a solar array simulator used in the Space Station independent verification program at the NASA Lewis Research Center. The hardware was modified to meet the functional requirements of the TROPIX spacecraft. However, the component ratings and sizes were larger than required. Also, this Phase I test bed simulated only one of the two SEP power channels.

The TROPIX test bed is a positive-ground design based on the series connected boost converter. The SCBC is used as the interface between the solar array simulator and the battery. A current regulator was added to the SCBC so the battery charge current would be controlled during insolation. The system is loaded using two large DC-DC converters (1kW each).

A control and data acquisition system developed for the Space Station test bed program was modified for use in the TROPIX EPS Test Bed. The complex, distributed, software control system developed for the Space Station test program was greatly simplified and implemented on a single desktop computer. Through the Operator Interface the test engineer can: turn the SCBC on and off, set current and voltage setpoints, and monitor the output voltage and battery current.

An orbital simulator was also developed for the TROPIX test bed. The orbital simulator accurately simulates any circular orbit using the facility control system and the solar array simulator. By entering several orbital parameters, the orbital simulator: calculates the orbit period, calculates max., min., and nominal eclipse times, and simulates the array heating following eclipse. The orbital simulator is an invaluable tool in evaluating power system performance through several orbits.

Series Connected Boost Converter

The SCBC used in the TROPIX EPS Test Bed is built around a 1kW zero voltage switching DC-DC

converter built by TRW of Redondo Beach, CA. It was designed to convert 120 Vdc to an isolated 28 Vdc for user loads on the Space Station[4]. The converter was modified to a positive ground, series connected boost converter to provide an output voltage range from -90 to -117 Vdc.

Initial development of the SCBC focused on providing output voltage regulation in a positive ground configuration. Since the voltage regulator is optically isolated from the power circuit, the positive ground configuration was trivial. The resulting SCBC had an output power capability of about 4.25 kW at an input voltage of 100 Vdc and an output voltage of 117 Vdc. The efficiency of the SCBC was measured using two calibrated Norma watt meters. The results are shown in Figure 4. The efficiency ranged from 95% to 98% and had an average efficiency of 96.4%. The efficiency numbers also include the control power since it is generated internal to the TRW ZVS converter.

Since the SCBC needed to control the charge current into the battery, a current control circuit was integrated with the existing voltage control circuit. The battery current is sensed (using a Hall effect sensor) and is compared to a reference. The current regulator adjusts the SCBC's boost voltage to control battery charge current. However, if the battery voltage reaches a pre-set maximum (defined by the voltage regulation setpoint) the converter reverts to a voltage regulation mode to protect the batteries from overcharging. The response of the current control circuit is 1 kHz and is much slower than the voltage control circuit.

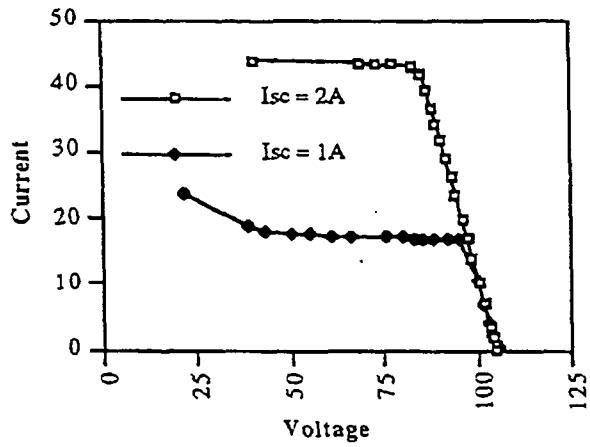

Figure 5 — Solar Array Simulator I-V Curve

Solar Array Simulator

The solar array simulator (SAS) was developed at Lewis to support testing of Space Station *Freedom* breadboard hardware and end-to-end system tests. It is an 82 string simulator which uses a large DC power supply and 82 linear power circuits to simulate the solar array I-V curve[5]. For the TROPIX EPS Test Bed, 24 strings of the simulator were re-wired for a positive ground configuration. The 24 circuits have a common positive bus and supply 24 separate return circuits. An adjustable short circuit current knob can reduce the power delivered by the SAS. The SAS I-V curve is shown in Figure 5 with the power supply, or Voc, set to 105 Vdc and I_{SC} set to 2A and 1A per string. Although the "knee" of the simulator is more pronounced than that of an actual array (see Figure 1), the SAS provides a realistic simulation for testing.

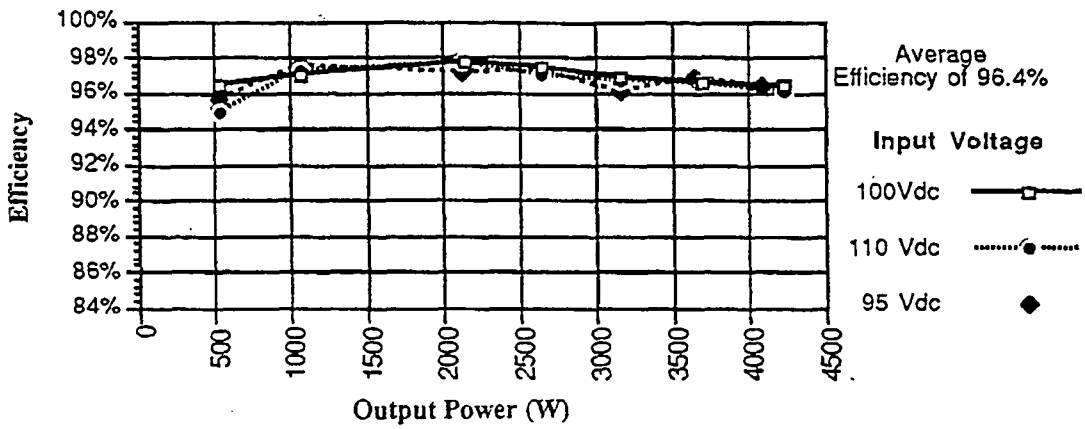

Figure 4 — Series Connected Boost Converter Efficiency Measurements

Battery Simulator

The battery simulator consists of eight (8) sealed, lead-acid batteries. Connected in series, they provide 90-117 Vdc and have a capacity of 80 A-hr. This battery simulator is not the appropriate size battery expected for the TROPIX satellite but was used since it was readily available.

Electrical Loads

The TROPIX Test Bed includes simulated user loads of the size and type expected on the spacecraft. By using realistic loads, not just laboratory resistive load banks, the system can be accurately evaluated for power quality and transient response. The same 1kW TRW ZVS isolating converter used for the SCBC is used as a bulk load converter. It converts the high voltage battery bus to 28 Vdc and isolates the loads from the positive ground. Connected to the output are several low power DC-DC converters of various sizes. Together they dissipate about 500 W through large power resistors mounted on a cold plate.

Another 1kW TRW ZVS isolating converter is used to simulate the response of one of the 900 W solar electric propulsion engines. The converter is loaded by a programmable load bank. The constant power DC-DC converter closely simulates the large signal dynamics of an SEP power processing unit (PPU). There are plans to incorporate an SEP PPU into the test bed in 1995 for complete system characterization.

System Test Results

The TROPIX EPS Test Bed has recently completed end-to-end integration and is currently undergoing system level tests. System tests planned include: power quality, efficiency, load transients, system faults, and orbital transition tests.

Results from the battery charge current regulator tests are shown in Figure 6. This test observed the battery voltage, battery charge current, and solar array simulator voltage over an 8.5 minute period as the SCBC charged the battery at a programmed level of 10A. During the charge period the system loading was varied several times to verify correct current regulation. Initial loading was 500W and the battery voltage was 90Vdc. For one minute the 500 W load was supplied by the battery and the charge current is -6.35 A (570 W delivered to the PPU simulator). At about one minute power was applied to the solar array simulator and the SCBC began to charge the battery at the 10 A setpoint level. During the next four (4) minutes the PPU load was varied from 900 W to 200 W while the battery charge current remained a steady 10 A. At about five (5) minutes the battery voltage had reached the maximum voltage setpoint of 116.7 Vdc and the battery current slowly tapered off as the voltage regulator gained control of the converter. During this time the PPU simulator load was still being varied but did not have an affect on the battery voltage or charge current.

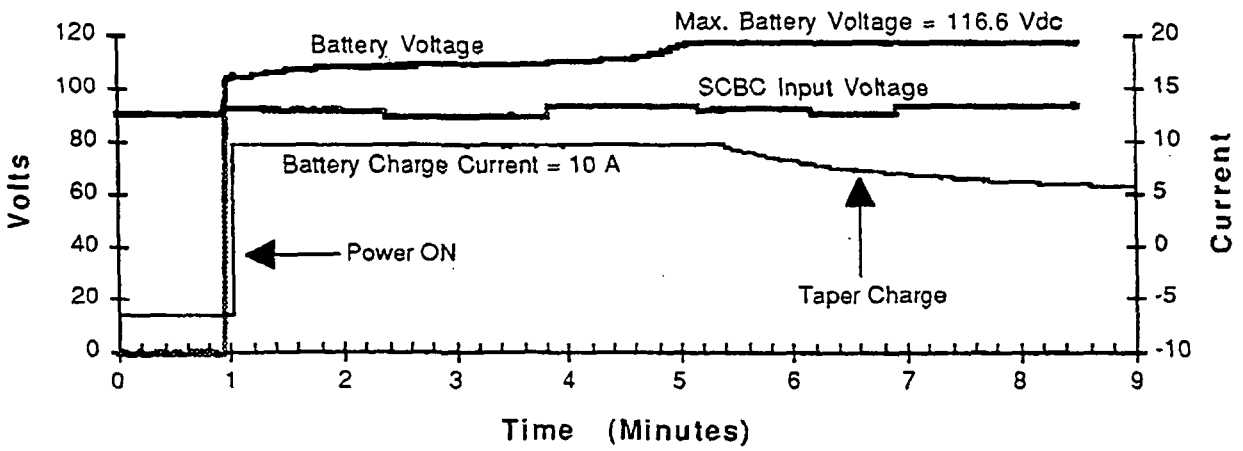

Figure 6 — Battery Charge Current Regulator Performance

PHOTOVOLTAIC REGULATOR KIT

Using the experience gained in the TROPIX EPS Test Bed, a concept has been developed which will improve small spacecraft power systems while also reducing development time and program costs. The concept is based on the series connected boost converter (SCBC) and involves development of a pre-engineered "kit" for fast and inexpensive development of an electric power system. This PV regulator kit is modular and can be easily paralleled to provide a range of power levels for small spacecraft power systems.

Description

A block diagram of the PV regulator kit concept is shown in Figure 7. The kit includes: a small housekeeping power supply, communications interface, input and output filters for improved power quality, a battery current monitor for charge control, and a bus voltage regulator and paralleling interface. The DC-DC converters used as the SCBCs can be any type of isolating power supply with an external interface for controlling output voltage. By not defining a specific DC-DC converter the kit can be used with almost any converter, including off-the-shelf commercial parts. This provides the EPS designer flexibility in the size of the power channel. Also, since DC-DC converters are used to power other spacecraft systems and experiment, a common converter can be used, further reducing EPS development costs.

Operation

The PV regulator is the interface between a properly sized solar array, a battery, and a secondary power bus. The first SCBC is controlled by the battery charge control circuit. By varying the SCBC boost voltage, the battery charge current can be controlled to follow a pre-defined profile. This profile can be controlled from an external computer or can be embedded in firmware in the communications interface. Should the DC-DC converter fail, current from the solar array will still charge the batteries.

The second SCBC is the interface between the battery bus and the secondary distribution bus. This converter supplies regulated voltage to the user loads which reduces their power converter complexity. This SCBC is controlled by the bus regulation controller which monitors the secondary bus voltage and adjusts the SCBC to keep the output voltage at a regulated setpoint value. The input and output filters are necessary to improve power quality and to isolate current and voltage ripple noise which might otherwise be passed directly to the user loads.

Not depicted in the block diagram is the fault protection system which consists of strategically placed fuses. Each SCBC has a fused input so that a fault in either DC-DC converter will not clamp the energy sources. Because the solar array is a current limited source, no fuse is needed to protect the wires from high fault currents. However, the battery can easily create large fault currents so the battery will be fused to protect against short circuits in the series connected boost wiring.

Modularity

The PV regulator kit is designed to be modular—allowing several units to be paralleled for greater

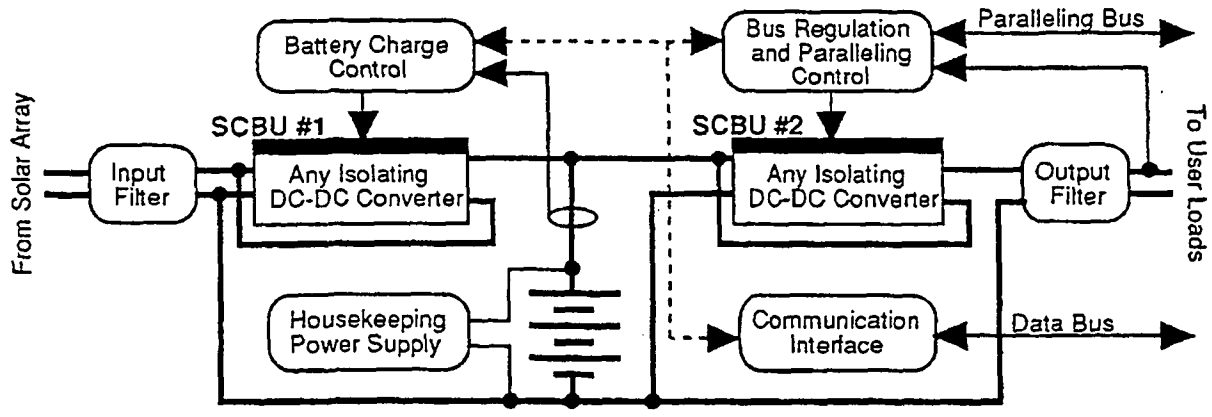

Figure 7 — Photovoltaic Regulator Kit Block Diagram

power delivery to the user loads. The paralleling is controlled through the regulated output bus and is an integral part of the bus regulation controller. Paralleling is accomplished through a shared signal bus which forces the converters to equalize their output currents with other units connected to the bus.

Flight Experiment

A version of the PV regulator kit is being developed for flight testing in the Small Spacecraft Technology Initiative (SSTI) program sponsored by NASA. Scheduled to fly in 1996, the SSTI satellite will test new technologies that can greatly impact the future costs and complexities of small spacecraft.

CONCLUSIONS

Based on the unique requirements of photovoltaic power systems, an optimal design can be achieved using the series connected boost converter (SCBC). The SCBC provides size, weight, power density, efficiency, fault tolerance, and commonality benefits over existing technologies. Also, electric power system development time and costs can be reduced by using commercial DC-DC converters as the SCBCs.

Development of the TROPIX EPS Test Bed has proven some of the benefits of the SCBC. Converter efficiencies of 95% to 98% have been measured in the lab. Use of the SCBC in a positive ground power system was also demonstrated. Further refinement of the test bed will focus on development of a Photovoltaic Regulator Kit. This pre-engineered power system element is modular and benefits from the SCBC technology. Future power systems can be "built" using off-the-shelf hardware—resulting in smaller, faster, and cheaper spacecraft.

ACKNOWLEDGMENTS

The author would like to acknowledge the work of Raymond Beach and Andy Brush in the development of the series connected boost converter.

REFERENCES

1 L. Trase, D. Fong, V. Adkins, A. Birchenough, "Description of the PMAD Systems Test Bed Facility and Data System", 27th Intersociety Energy Conversion Engineering Conference, San Diego, CA, August 1992.

2 R.F. Beach, A.S. Brush, "Series Connected Converter for Control of Multi-Bus Spacecraft Power Utility", NASA Disclosure of Invention, #LEW15918-1C, Nov 1993.

3 J. Mark Hickman, "Solar Electric Propulsion for Magnetospheric Mapping", 30th AIAA/ASME/SAE/ASEE Joint Propulsion Conference, June 27-29, 1994.

4 R. Lebron, "Load Converter Interactions with the Secondary System in the Space Station Freedom PMAD DC Test Bed", 27th Intersociety Energy Conversion Engineering Conference, San Diego, CA, August 1992.

5 T. Vasek, A. Birchenough, "Development of a Ninety String Solar Array Simulator", 26th Intersociety Energy Conversion Engineering Conference, Boston, MA, August 1991.

Appendix 4 - CAFE

CLOUD AND FEATURE EDITING (CAFE)
TECHNOLOGY DEMONSTRATION EXPERIMENT FOR LEWIS SSTI SPACECRAFT

PROGRESS/STATUS REPORT 4 OCTOBER, 1995

BACKGROUND:
The purpose of the Cloud and Feature Editing (CAFE) experiment for the TRW Lewis SSTI Spacecraft is to perform on-ground non real-time evaluation of algorithm concepts for detecting cloud presence in multispectral Earth resource imagery. The ultimate goal of this research is to develop methods and refine concepts, for autonomous use aboard future resource satellites, of detecting cloud-contaminated imagery in real-time and suppressing its transmission to Earth. Major economies in resource satellite data archival should thereby be realizable. Data from the TRW Hyperspectral Imager (HSI) will be used to develop and test these concepts.

ASSUMPTIONS:
To evaluate autonomous cloud-detection with an HSI-class instrument, it was assumed that no ancillary data as, e.g., from thermal infrared spectral channels carried aboard weather satellites, would be available. Therefore, the CAFE experiment will use only the channels available for HSI. This, of course, means that CAFE will not work at night. Also, a definite bias was adopted, of regarding clouds as a contaminant, and not as items of investigation. This means, for example, that we are only interested in whether a pixel is obscured/not obscured by cloud, and not in the cloud type, altitude, ice content, etc.

ALGORITHM APPROACHES:
A comprehensive literature search was performed in-house for cloud detection/editing techniques. The results of this search pointed up the fact that a wide variety of techniques exists. The majority of them, however, deal with the study of the clouds themselves, as for climatological research purposes. Then, too, few of these techniques were judged feasible for real-time application aboard a small satellite. Simple,practical, flexible, and robust approaches are what is needed for SSTI. Consultation with researchers in the field continues to indicate that a perfect performance under all conditions , and over all types of terrain backgrounds, is still not achievable at this time. Therefore, our goal for SSTI is a high percentage of success, but not necessarily a perfect performance in detecting cloud obscuration under all circumstances. In trading off algorithm approaches, increase in accuracy will be traded off against increase in complexity. Figures of merit, such as success, failure, and false alarm rates will be used as the performance metrics in these tradeoffs. The results of the above procedure resulted in three CAFE algorithms, which are being evaluated for the Lewis SSTI, as follows:

1. THE ORIGINAL APPROACH FOR LEWIS (ADVANCED FILE CONCEPT):
This approach is based on the Feature identification and Location Experiment (FILE), developed by Martin-Marietta and NASA-Langley and flown successfully aboard the Space Shuttle and research aircraft during the 1980s. The approach is relatively simple to implement. It uses ratios of the radiometer signal values in the 0.65 and 0.85μm channels, together with threshold signal values in those channels, in a linear discriminant function algorithm, to classify a scene as bare land, water, vegetation, or as a member of the class cloud-snow-ice. (Note that this two-channel-only approach is the one being used for the Clark SSTI mission; the limited number of spectral channels available for Clark made this approach the only practical choice.) For Lewis SSTI, however, the wide spectral range and large number of spectral channels afforded by the HSI allows a more advanced version of FILE to be utilized, and more "spectrally rich" algorithms generally to be tested. Therefore, two more channels were added, 1.25 and 1.55 μm -- for identifying clouds, snow, and ice separately. You may recall that this "advanced FILE" four channel approach (0.65, 0.85, 1.25, and 1.55 μm) was our original concept in the summer of 1994, when we "signed on" to SSTI. This concept remains as one of the three being evaluated. A slight elaboration on this approach is also being evaluated. This adds two additional channels -- 1.38 and 1.88 μm (recommended by Dr. Gao, see below)-- as a pre-filter to detect high altitude cloud cover. (You may recall that I was starting to advocate this addition at the time of the ICDA back in January, 1995.) Apparent reflectance values are determined in these two new channels. The 1.38 μm channel is used at latitudes below 50 degrees; the 1.88 μm channel is used at higher latitudes. The computation of apparent reflectance is an additional complication, but it may be worth it in terms of quickly identifying extensive areas of high-altitude cloud cover, and thereby speeding the clouded-data rejection process.

REFLECTANCE-BASED APPROACHES:
Early in 1995, through contacts with Langley's Atmospheric Sciences Division, we became aware of some research into cloud detection being performed by Dr. Bo-Cai Gao of the University of Maryland, working at NASA-Goddard. Dr. Gao has done considerable analysis of AVIRIS multispectral data to develop methods for detecting clouds over all kinds of background surfaces, and has found several useful relationships of the data from various AVIRIS channels. We decided to develop additional CAFE algorithms, based on Gao's research, for several reasons:

-- AVIRIS, developed by TRW for JPL, has similar spectral range and channel content to HSI. Conclusions based on analysis of AVIRIS data may be readily applicable to HSI-based CAFE algorithms.

--Gao's cloud detection techniques are based on thresholds and

ratios of apparent reflectances, rather than on signal ratios, as in FILE. The reflectance-based approach may offer additional physical insight to the radiative transfer of the scene, i.e., into what kinds of surfaces are contributing. The tradeoff here is the need to determine apparent reflectance. This requires knowledge of the solar zenith angle, and the modeling of exoatmospheric solar irradiance in the algorithms. However, the additional complexity may be well worth it, if we get more accurate results and more reliable cloud detection. Testing on real data will determine whether the additional complexity is "worth it".

-- The fact that we are not a real-time experiment gives us the chance to analyze and reanalyze the multispectral data with a variety of CAFE techniques. Therefore, a "more complicated" approach, such as Gao's, is feasible to evaluate in this context.

For all the above reasons, we decided to add a "Gao-based" algorithm to the CAFE suite, and to evaluate it alongside the FILE-based one, using the HSI data.

2. TEN-CHANNEL CAFE ALGORITHM:
Adaption of Gao's ideas resulted in a ten-channel, several-tier approach, outlined roughly as follows:

-- Determine the reflectance in the 1.38 or 1.88 μm channel, depending on latitude, as described above. If the reflectance is above the threshold, classify the pixel as cloud-obscured and go to next pixel. Otherwise, analyze the pixel further in the other channels.

-- Use the 0.66 and 0.86 μm channel reflectances, and the Normalized Difference Vegetation Index (NDVI) to classify a pixel as water, vegetation, etc.

-- Use the 2.13 and 0.86 μm channel data to discriminate clouds from ice and snow.

--(Grafted in from the Advanced FILE concept). Use the 1.25 and 1.55 μm channel data, along with the 0.66 μm data, to determine snow or ice.)

-- (Still experimental) Use 0.94 and 1.04 μm data for more reliable detection of clouds over bare land.

-- (experimental) Use 1.6 μm channel for an alternate, possibly better discrimination of cloud and ice. (This may supplant the 1.55 μm channel in this role).

At this date, the logic utilizing data from the 0.94, 1.04, and 1.60 μm channels is not yet "wired in"; we are still experimenting with it. All the other channels are already part of

this logic , however.

3. STREAMLINED, CLOUD/NO-CLOUD DETECTION ONLY APPROACH:
This approach is a streamlined version of approach no. 2, with all feature identification removed, save that for detecting clouds' presence or absence. This streamlined approach may be of interest to some users. In any event, the results of this approach should provide a "report card" on our performance on our primary task--the detection of cloud-contaminated imagery--uncomplicated by the identification of surface background types.

CURRENT STATUS/PLANS:

At the present time, all three algorithms described above have been coded in "C" , and tested and debugged on synthetic radiance data. The synthetic radiance data were generated by me using the MODTRAN atmospheric radiative transfer program. Twenty-two background reflectance scenarios, cloud-filled and cloud-free, and with varying amounts of atmospheric haze, were used in the simulation base. Radiance data were computed for each of the ten spectral channels noted in algorithm 2, for each of the scenarios. Initial testing shows that all three algorithms detect clouds very well, albeit not perfectly. Much more simulation is needed. Additional simulation, using synthetic data, is planned, but the real test will take place when we try the algorithms on AVIRIS data. We hope to start testing this fall on real data.

It should be noted that all our algorithms include an instrument model. We model instrument optical and radiometric response, and the signal-bit conversion process. At present, we do not have numbers from you for optical and instrument response; we are using placeholder, or "1.00" values for these quantities. Upon receipt from you of final values, we will incorporate them into our model.

Richard E. Davis

(804)864-1647

REPORT DOCUMENTATION PAGE

QMB No. 0704-0188

1. AGENCY USE ONLY (Leave blank)	2. REPORT DATE	3. REPORT TYPE AND DATES COVERED
	24 October 95	Bi-annual January 95 thru June 95

4. TITLE AND SUBTITLE
Technology Report

5. FUNDING NUMBERS
Contract NASW-4945

6. AUTHOR(S)
George Reppucci, SSTI Program Manager

7. PERFORMING ORGANIZATION NAME(S) AND ADDRESS(ES)
SSTI Program
TRW Inc.
One Space Park M2/2120
Redondo Beach, CA 90278

8. PERFORMING ORGANIZATION REPORT NUMBER
Space and Technology Division, F.6.b

9. SPONSORING/MONITORING AGENCY NAME(S) AND ADDRESS(ES)

10. SPONSORING/MONITORING AGENCY REPORT NUMBER
INTERIM
IN-18-CR
5614

11. SUPPLEMENTARY NOTES
None

3CIT
p-36

12a. DISTRIBUTION/AVAILABILITY STATEMENT
See Handbook NHB 2200.2

12b. DISTRIBUTION CODE

13. ABSTRACT (Maximum 200 words)

This is the second in a series of semi-annual reports that describe the technology areas being advanced under this contract and the progress achieved to date. The last technology report concentrated on the spacecraft. This report places greater emphasis on the payloads. White papers by several of the payload providers are attached. These are HSI, UCB, PRKE and CAFE. This report covers the period from January 1995 through June 1995.

14. SUBJECT TERMS
Critical Design Audit, CDA, Final Design, Subsystem Fabrication Phase

15. NUMBER OF PAGES

16. PRICE CODE

17. SECURITY CLASSIFICATION OF REPORT	18. SECURITY CLASSIFICATION OF THIS PAGE.	19. SECURITY CLASSIFICATION OF ABSTRACT	20. LIMITATION OF ABSTRACT
Unclassified	Unclassified	Unclassified	SAR

SN 7540-01-280-5500